*Journal of the Geological Society, London*, Vol. **167**, 2010, pp. 11–20. doi: 10.1144/0016-76492009-109.

# Jurassic geothermal landscapes and fossil ecosystems at San Agustín, Patagonia, Argentina

DIEGO M. GUIDO[1], ALAN CHANNING[2], KATHLEEN A. CAMPBELL[3]* & ALBA ZAMUNER[4]

[1]*CONICET-UNLP, Instituto de Recursos Minerales, Calle 64 esquina 120, La Plata (1900), Argentina*

[2]*School of Earth and Ocean Sciences, Cardiff University, Main Building, Park Place, Cardiff CF10 3YE, UK*

[3]*School of Environment, University of Auckland, Private Bag 92019, Auckland 1142, New Zealand*

[4]*Departamento de Paleobotánica, Facultad de Ciencias Naturales y Museo-UNLP, Paseo del Bosque (1900), La Plata, Argentina*

**Corresponding author (e-mail: ka.campbell@auckland.ac.nz)*

**Abstract:** An extensive, well-preserved, Late Jurassic (*c*. 150 Ma) geothermal system at San Agustín farm in the Deseado Massif, Patagonia, Argentina, is described. This deposit, along with others previously known from the same region, partially fills a considerable gap between Cenozoic and scattered Palaeozoic hot spring localities reported worldwide. The San Agustín deposit is novel because it represents a large (1.4 $km^2$) and nearly complete geothermal landscape. Siliceous hot spring facies, both subaerial and subaqueous, are exposed side by side in their original spatial and geological context, set amongst intrusive rhyolite domes and fluviolacustrine sediments. The Jurassic hot springs have preserved an entire local ecosystem containing microbes, arthropods, gastropods and plants exhibiting Lagerstätten-style preservation. Plant preservation, in particular, ranges from decayed litter, to seedling sprouts, and to dense stands in life orientation with intact anatomy. The San Agustín deposit shares some ecological, taphonomic and sedimentological characteristics with modern hot springs. As it formed in a pre-angiosperm world, it is akin to the famous hot spring-related Devonian Rhynie cherts of Scotland. It differs in having excellent exposure, and thus will probably contribute to a better understanding of biosignal preservation in extreme environments in the geological record.

Terrestrial hot spring deposits are prized by geologists as potential indicators of precious metals mineralization (Sillitoe 1993) or geothermal reservoirs at depth. Palaeontologists and biologists use them as analogue settings for early life on Earth (e.g. Shock 1996; Stetter 1996; Farmer 2000; Konhauser *et al*. 2001). These unusual deposits are derived from hydrothermal fluids that typically precipitate silica or carbonate minerals at the Earth's surface (at $\leqslant$100 °C) where the water table intersects topography (see Sillitoe 1993). They generally develop in volcanically active areas within dynamic tectonosedimentary settings, which results in their variable preservation potential (White *et al*. 1989; Simmons *et al*. 1993). Hot spring deposits can rapidly entomb individual organisms and even complete ecosystems within spring-deposited minerals. These often record physicochemical signatures of the original habitat (e.g. Cady & Farmer 1996; Trewin 1996; Farmer 2000). In rare circumstances, cellular details of soft tissues, or the anatomy of entire organisms, are preserved in 'Konservat-Lagerstätten' deposits, such as the well-known Early Devonian (*c*. 396 Ma), hot spring-related Rhynie cherts of Scotland (Rice & Trewin 1988; Trewin 2001; Trewin & Rice 2004). Rhynie fossils have been used to assess early terrestrial ecosystem composition (Anderson & Trewin 2003; Trewin 2001; Trewin & Rice 2004), functioning of early land plants (Edwards *et al.* 1998) and animals (Shear & Selden 2001), key biotic divergence points (e.g. Engel & Grimaldi 2004; Taylor & Berbee 2006), and broader evolutionary patterns (Kenrick & Crane 1997). Despite their significance, the geological and geographical context of the Rhynie cherts is largely extrapolated from subsurface drilling because of a lack of outcrops.

In contrast, the Late Jurassic siliceous hot spring deposit (sinter; 1.4 $km^2$) at San Agustín, described for the first time herein, is well exposed and nearly undisturbed geologically (Figs 1 and 2). In places, microbes, arthropods, gastropods and plants also show the rare phenomenon of exceptional preservation in the fossil record (e.g. Figs 3–5), as outlined further below.

## Regional geological context

The San Agustín geothermal system occurs within the Deseado Massif, a 60 000 $km^2$ geological province of southern Patagonia characterized by extensive (>30 000 $km^2$), bimodal volcanism of the Bahía Laura Group, including calc-alkaline rhyolites, minor andesites and rare dacites. These rocks are part of the Chon Aike Large Igneous Province (Pankhurst *et al*. 1998), which delineates the commencement of supercontinent break-up owing to slow subduction rates at the Pacific margin of Gondwana and a mantle plume active in the Jurassic (177.8–150.6 Ma; Pankhurst *et al*. 2000; Riley *et al*. 2001). During late Bahía Laura volcanism (Late Jurassic), extension and a high thermal gradient in the back-arc produced hydrothermal mineralization including economic gold- and silver-bearing epithermal deposits, and several hot spring occurrences mainly in the western areas of the province (Fig. 1a; Guido & Schalamuk 2003). These comprise mostly travertines, some siliceous sinters and geothermally related cherts that are hosted in tuffs, breccias, and reworked volcaniclastic sediments within fluviolacustrine settings (Schalamuk *et al*. 1997, 1999*a*; Marchionni *et al*. 1999; Guido *et al*. 2002; Echeveste 2005; Channing *et al*. 2007; Guido & Campbell 2009). The Deseado Massif hot spring deposits partially fill a gap in the geological record between well-known Cenozoic (Sillitoe 1993) and scattered

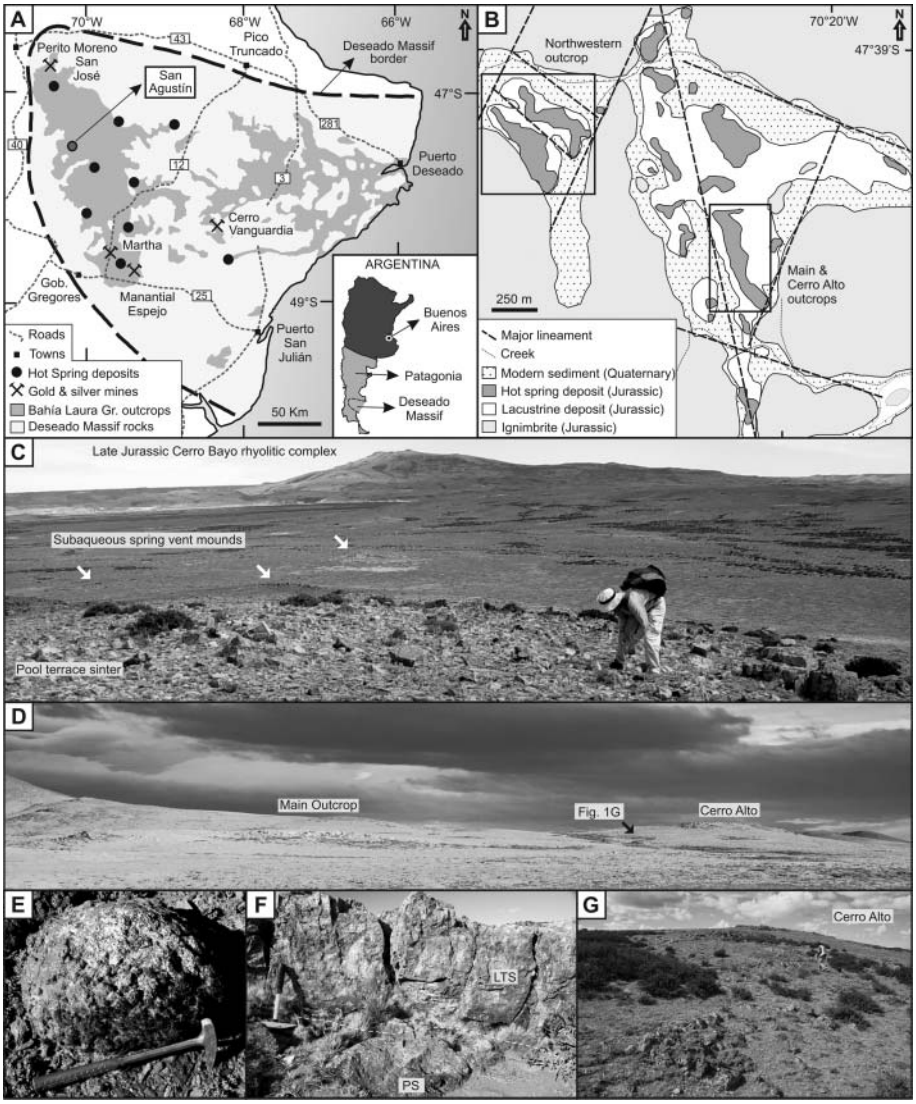


**Fig. 1.** Geological maps, field site overview and typical outcrop images of the San Agustín deposit. (**a**) Simplified geological map of the Deseado Massif, with hot spring occurrences and Au–Ag mines indicated. (**b**) Geological map of the San Agustín study site showing volcano-sedimentary setting, and locations of the detailed facies and structural maps of Figure 2. (**c**) Northwestern outcrop overview from top of pool sinter terrace, a palaeotopographic high (compare Fig. 2a and c), with arrows over some of the subaqueous caddis-fly–microbial mounds in the topographically lower, lacustrine spring vent mound area. Penecontemporaneous Late Jurassic rhyolite dome, Cerro Bayo, in distance. View to the WNW. (**d**) Main outcrop and Cerro Alto sinter aprons (compare Fig. 2b and f); view to the SE. (**e**) Subaqueous spring vent bioherm comprising hemispheroidal, botryoidal microbialite (exterior surface) and fossil tubes (interior, not visible) in a lacustrine setting. Northwestern outcrop area. (**f**) Thinly layered, inferred low-temperature sinter (LTS) overlying a palaeosol (PS) with sinter fragments (compare Fig. 2h). Northwestern outcrop. (**g**) Typical low-lying, plant-rich chert outcrops exposed in a palaeolow area between the Main and Cerro Alto sinter terraces.

Palaeozoic (e.g. Cunneen & Sillitoe 1989; White *et al*. 1989; Rice *et al*. 1995; Walter *et al*. 1996) examples. The Jurassic Patagonian rocks were buried by Cretaceous and Cenozoic continental and marine passive margin successions, and subsequently unearthed with minimal structural disturbance to expose intact erosional windows into an exhumed fossil landscape, at present revealed in a NNW–SSE-oriented, 240 km × 100 km area of surface epithermal deposits (Fig. 1a).

**Fig. 2.** Key structural and facies associations, and representative sedimentary fabrics of the San Agustín geothermal system, with some comparative modern analogue textures from hot springs of the Taupo Volcanic Zone, New Zealand. (**a**) Northwestern outcrop area comprising subaqueous spring vent mounds in palaeolow lake areas, and adjacent, palaeotopographically higher, subaerial sinter terraces. (**b**) Subaerial sinter aprons at Cerro Alto and Main outcrop areas, adjacent to cooler, topographically lower, plant-rich, geothermally influenced wetlands, ponds and lake shoreline facies. (**c**) Schematic SW–NE cross-section (location shown in (**a**)), showing spatial associations between faults, sinter aprons and lacustrine spring vent mounds. Northwestern outcrop area. (**d**) Bioherm cut slab revealing botryoidal microbial laminites encrusting radiating tube clusters of spring vent mound facies. Vertical section view; Northwestern outcrop area. (**e**) 'Pool mat' terrace sinter, showing tufted, undulatory and convoluted horizons with high primary porosity. Vertical section view; Northwestern outcrop area. (**f**) Schematic NW–SE cross-section (location shown in (**b**)). Main outcrop and Cerro Alto sinter-apron areas. (**g**) Sinter with conifer branch fragment revealing 3D details of periderm morphology and wood anatomy. Northern Main outcrop. (**h**) Sinter fragments in palaeosol (compare Fig. 1f). Northern Main outcrop. (**i**) Mid-temperature sinter, displaying wavy laminae and lenticular voids inferred to be microbial mat-generated gas bubbles. Vertical section view; Main outcrop. (**j**) Cross-section through dense, vertical stands of sphenophytes in life position from the geothermal pond facies. Western Cerro Alto outcrop. (**k**) Dark grey, varved lacustrine siltstone overlain by crenulated, light–dark laminae interpreted as microbial fabric. Vertical section view. Lake shoreline transition, location 1 km ENE of Main outcrop. (**l**) Plant fragments and seedlings in the lake shoreline facies; dark, crenulated laminae and clots are inferred to be microbial in origin; 1 km ENE of Main outcrop. (**m**) Irregular, contorted, ropy fabric typical of 'pool mat' sinter areas. Oblique vertical section view; Northwestern outcrop. (**n**) Curled, contorted, drying mats from a modern mid-temperature sinter apron at Orakei Korako, Taupo Volcanic Zone. Plan view. (**o**) Streamer fabric of finely filamentous sinter. Bedding plane view; Northwestern outcrop. (**p**) Modern streamer fabric in shallow, mid-temperature, hot spring discharge channel, Orakei Korako (Taupo Volcanic Zone). Plan view.

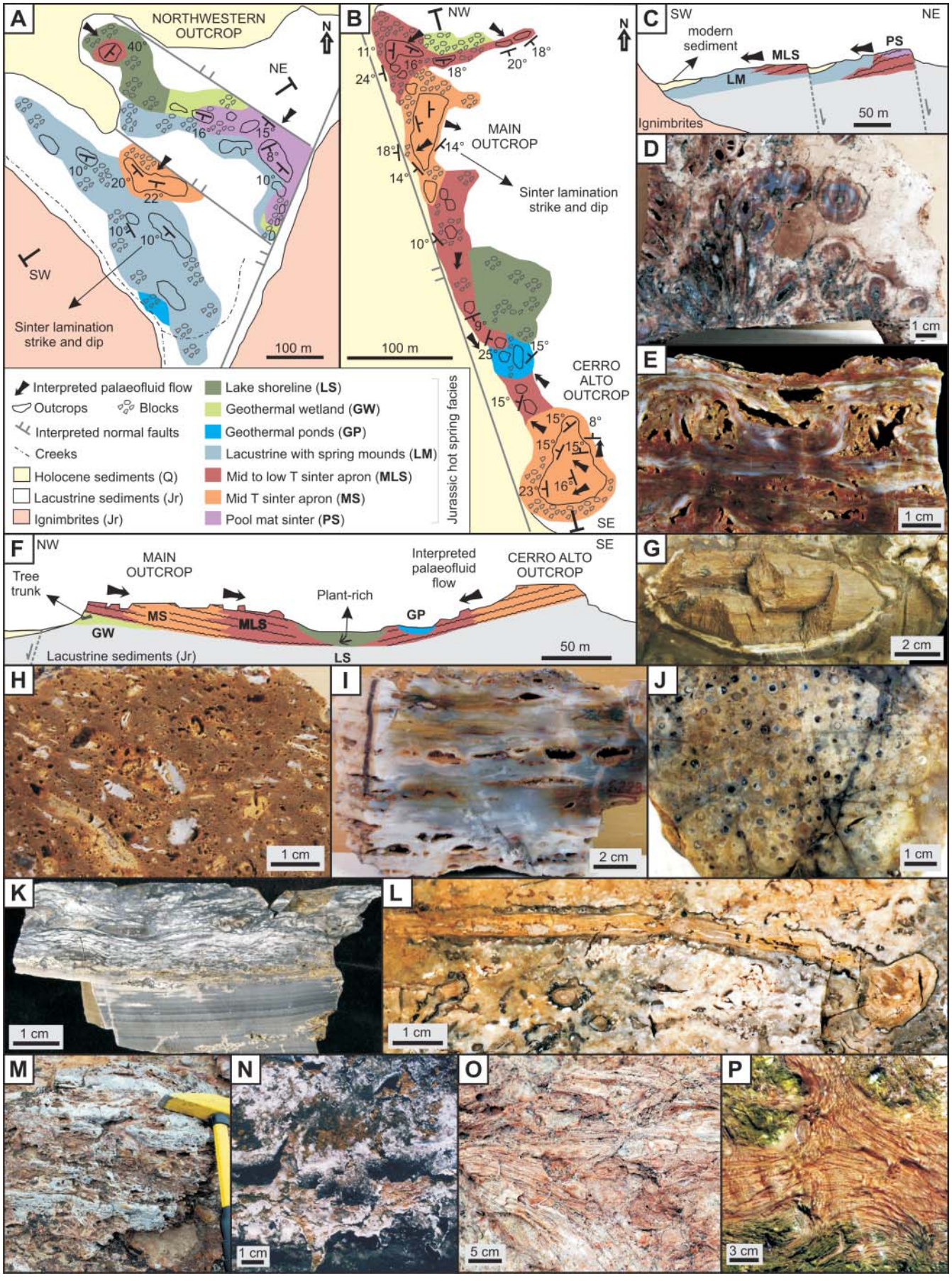
A
NORTHWESTERN OUTCROP
N
NE
SW
Sinter lamination strike and dip
100 m
B
NW
N
MAIN OUTCROP
Sinter lamination strike and dip
100 m
CERRO ALTO OUTCROP
SE
C
SW
NE
modern sediment
MLS
PS
LM
Ignimbrites
50 m
D
1 cm
E
1 cm
Interpreted palaeofluid flow
Outcrops
Blocks
Interpreted normal faults
Creeks
Holocene sediments (Q)
Lacustrine sediments (Jr)
Ignimbrites (Jr)
Lake shoreline (LS)
Geothermal wetland (GW)
Geothermal ponds (GP)
Lacustrine with spring mounds (LM)
Mid to low T sinter apron (MLS)
Mid T sinter apron (MS)
Pool mat sinter (PS)
Jurassic hot spring facies
F
NW
SE
Tree trunk
MAIN OUTCROP
Plant-rich
Interpreted palaeofluid flow
CERRO ALTO OUTCROP
MS
MLS
GP
GW
Lacustrine sediments (Jr)
LS
50 m
G
2 cm
H
1 cm
I
2 cm
J
1 cm
K
1 cm
L
1 cm
M
N
1 cm
O
5 cm
P
3 cm

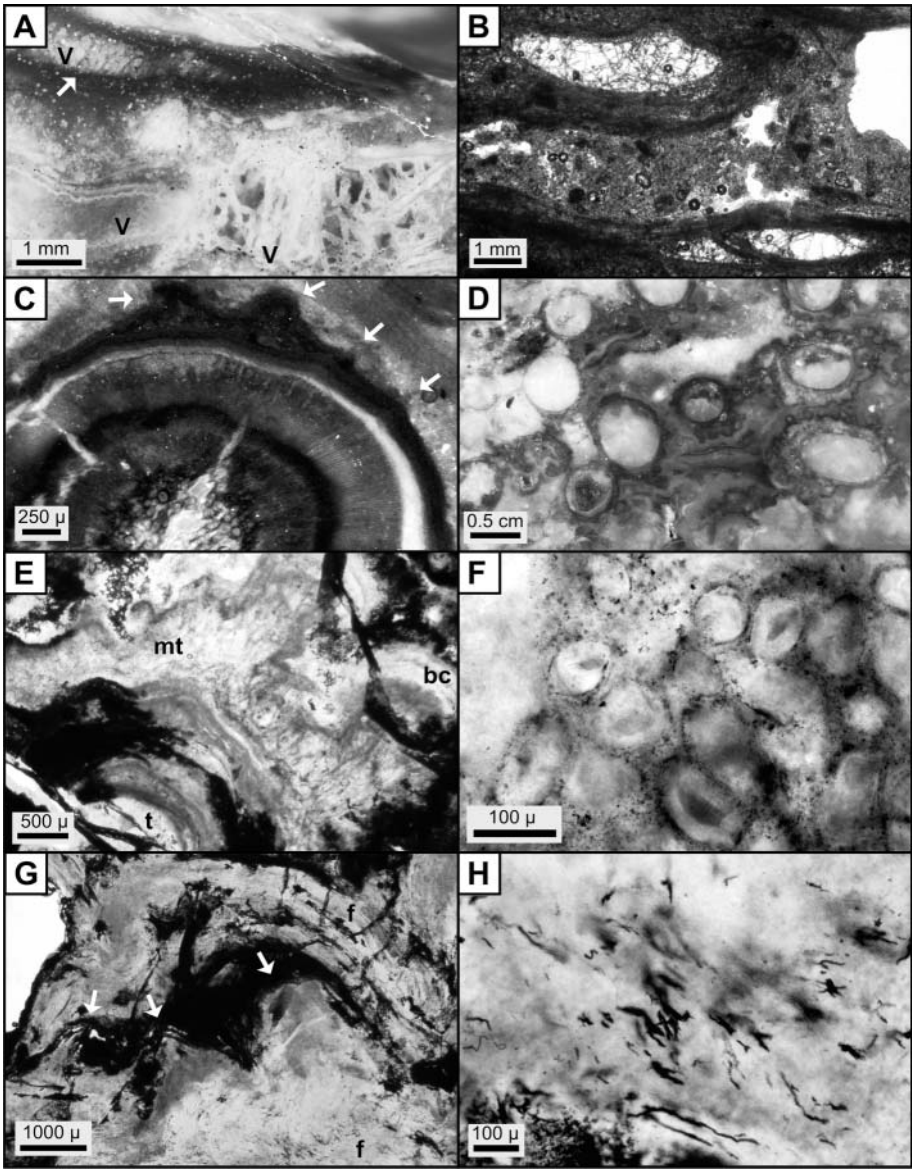


**Fig. 3.** Detail of microbial fabric preservation in the San Agustín geothermal system, with some similar fabrics from Pleistocene sinters of New Zealand shown for comparison. (**a**) Densely packed, brown, vertical filaments (arrow) filling a lenticular void within a dark, organic-rich (?) horizon. White, silica-encrusted filaments also partially fill a lenticular void, or trapped gas bubble (lower right). V, void. Vertical section view; Main sinter outcrop. (**b**) Silicified filaments that grew into voids formed by photosynthetic degassing in a *c*. 15 ka old microbial mat of the Tahunaatara sinter, Taupo Volcanic Zone, New Zealand. Vertical section view. (**c**) Woody stem or branch of unidentified conifer (2 years old) showing central pith with encrusting microbial laminae with tufted surface projections (arrows). Transverse section view; 1 km ENE of Main outcrop. (**d**) Bioherm detail of caddis-fly pupal or larval cases (circular, white, micro-quartz fillings) concentrically overgrown by microstromatolites (dark brown linings and digitate projections). Transverse section view; Northwestern outcrop. (**e**) Cross-section detail of botryoidal, 'cauliflower,' microbial fabric (bc) comprising microtubules (mt, in vertical orientation radiating away from tube) and encrusting caddis-fly larval tube (t) in the spring vent mound facies. (**f**) Detail of microtubules (compare (**e**)) in cross-section. (**g**) Conical microbial tuft overgrowing three smaller cones (arrows), constructed of filaments (f) in parallel laminated or vertical tufted orientations. Vertical section view; 'pool mat' sinter facies. (**h**) Detail of laminae of conical tufts (compare (**g**)) constituting silicified, orange to red–brown filaments (Fe-stained or organic residue?). 'Pool mat' sinter facies.

## An overview of the stratigraphic and structural associations within the San Agustín deposit

The San Agustín deposit is located on the western border of the Deseado Massif province. The geothermal complex is positioned stratigraphically at the top of a sequence of extensive, silicified lacustrine deposits (>30 km$^2$) that filled fault-related Jurassic valleys of a largely ignimbritic volcanic terrain (Fig. 1b). These sedimentary deposits are located on a regional WNW–ESE fault that links the sinter with the Late Jurassic Cerro Bayo rhyolitic complex (Fig. 1c), located *c*. 7 km to the NW. Furthermore, in the same lineament but 20 km to the SE large travertine deposits have been described by Marchionni *et al*. (1999). Faults were active during and following hydrothermal activity, and some appear to have channelled geothermal fluid up-flow during the Late Jurassic. The San Agustín siliceous sinter outcrops, originally opaline and later replaced by finely crystalline quartz, are clearly controlled by the regional WNW–ESE fault with cross-cutting NNW–SSE- and NE–SW-oriented lineaments (Fig. 1b). We mapped in detail the structure and sedimentary facies of the most extensive and best preserved hot spring-related deposits: the Northwestern, Main and Cerro Alto outcrops (Figs 1 and 2). They reveal palaeoflow directions, and original lateral and vertical relationships between the various facies types, as defined below.

The Northwestern outcrop (Figs 1b, c, e and 2a, c) is characterized by subaqueous spring vent mounds, subaerial sinter aprons including some with deep pools, and several geothermally fed, cooler, wet 'margin' settings. Palaeofluid flow generally was towards the SW (Fig. 2a), as measured by strikes and dips of coherent sinter laminae. The sequence was tilted 10° to the SW in relation to the dip of surrounding lacustrine sediments, and relatively displaced by two minor normal faults (Fig. 2c). A second hydrothermal fluid source from the NW is also evident at the northernmost portion of this outcrop (Fig. 2a), where a mid- to low-temperature sinter apron exhibits a lateral transition into a geothermal wetland and lake shoreline facies with plant-rich chert.

The Main outcrop and Cerro Alto (Figs 1b, d, f, g and 2b, f)

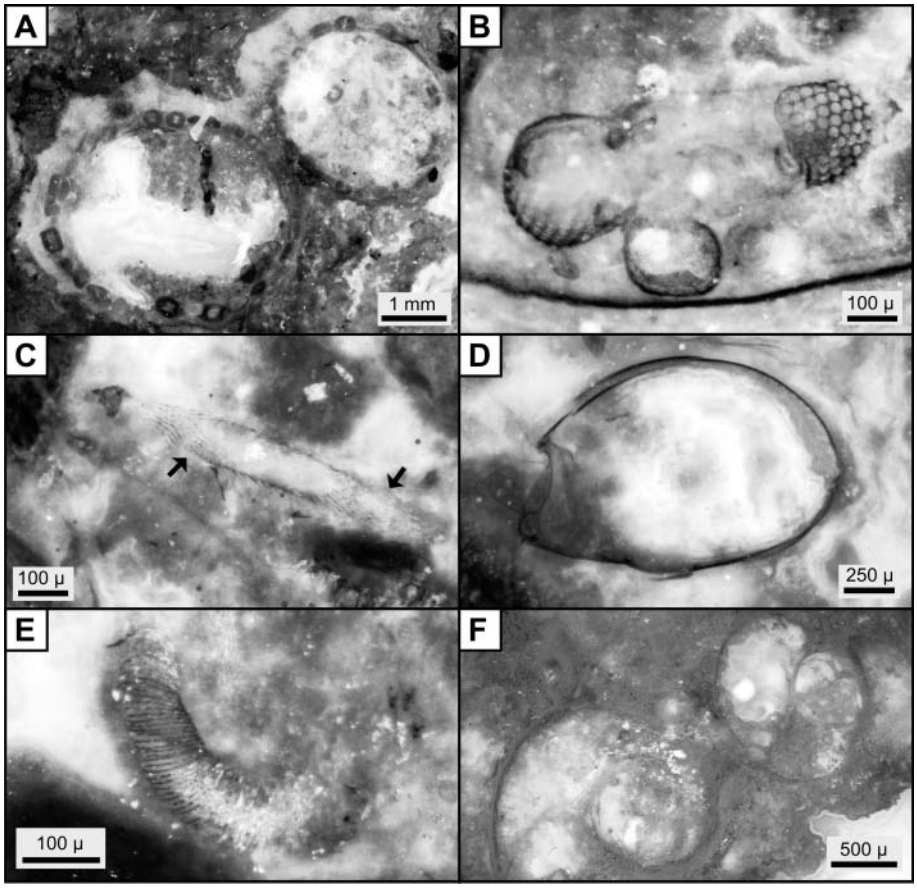


**Fig. 4.** Examples of some of the metazoan fossils preserved in the San Agustín geothermal system. (**a**) Detail of caddis-fly pupal or larval cases lined by well-preserved (?)crustacean coprolites with central lumen; 1 km ENE of Main outcrop. (**b**) Compound eyes of presumed aquatic arthropod in microcoprolite-rich fabric. Northern Main outcrop. (**c**) Bristles (arrows) of disarticulated arthropod appendage. Northern Main outcrop. (**d**) Carapace cross-section of *Triops*-like aquatic crustacean. Northern Main outcrop. (**e**) Possible articulated abdomen segments of a *Triops*-like aquatic crustacean. Northern Main outcrop. (**f**) Gastropods preserved amongst stromatolitic botryoids. Northwestern outcrop.

represent two subaerial sinter-apron deposits 500 m to the SE of the Northwestern outcrop. Two source areas from the north and south, respectively, are implied, with hot springs discharging over aprons dipping 15° towards a central area of geothermally influenced, plant-rich facies accumulating along cooler, wet apron margins (Figs 1g and 2f). In distal margin areas, laterally discontinuous lenses of silicified fluviolacustrine sediments within plant-rich chert beds imply interfingering of lake shoreline and geothermal wetland settings. The northern portion of the Main outcrop (Fig. 2b) contains sinter with *in situ* tree stumps and fallen and partially decayed logs and branches (e.g. Fig. 2g). This overlies a palaeosol packed with sinter fragments (Figs 1f and 2h), indicating hot spring encroachment into a nearby standing conifer forest.

## San Agustín hot spring palaeoenvironments

Studies of modern hot spring analogues for the San Agustín geothermal system (e.g. at Yellowstone National Park, Wyoming, USA, and the Taupo Volcanic Zone, New Zealand) have revealed the physical and chemical conditions under which their biota are partitioned, and biosedimentological fabrics diagnostic of various subenvironments. These broadly track temperature and pH gradients from spring vent sources (*c*. 100 °C) to distal discharge areas and geothermal wetlands (*c*. 40 °C to ambient) (see Cady & Farmer 1996; Jones *et al*. 1998; Channing *et al*. 2004; Channing & Edwards 2009). Based on comparative data, seven hot spring-related sedimentary facies, with particular stratigraphic, sedimentological and palaeontological attributes (see Cady & Farmer 1996; Trewin 1996; Walter *et al*. 1996; Farmer 2000; Campbell *et al*. 2001; Trewin *et al*. 2003; Fayers & Trewin 2004; Channing & Edwards 2009), were identified at San Agustín (Figs 1–5). Some are inferred to have formed in perennially wet conditions (subaqueous spring vents, geothermally influenced wetland, lake shoreline facies). Others indicate intermittently wet and dry, sinter-apron terrace deposits ('pool mat' sinter, mid-temperature sinter, mid- to low-temperature sinter, supra-apron geothermal ponds). Inferred facies relationships of the San Agustín geothermal system are summarized in the schematic box diagram of Figure 6.

Microbial–caddis-fly bioherms (0.3–1.5 m in diameter; Fig. 1e) developed in low-lying areas where lake sediments accumulated around active subaqueous spring vents (Figs 1c, 2a, c, and 6). They constitute dense aggregations of radiating, silicified, caddis-fly pupal or larval tubes (5–10 mm diameter), constructed from faecal pellets, degraded plant fragments, ostracodes and rock fragments (Fig. 4a). Digitate microstromatolites coat single tubes and merge into larger botryoidal, 'cauliflower' stromatolites (Figs 2d and 3d–f). Densely packed microtubules constructed the stromatolitic fabrics, similar to radiating filament moulds preserved in Great Salt Lake microbial mounds of Utah (Halley 1976, fig. 6). Gastropods (Fig. 4f) preserved between tubes in the San Agustín mounds were probably grazers upon the microbial mats. Similar bioherms have been reported from Early Cretaceous lacustrine deposits of Korea (Paik 2005) and the Eocene Green River Formation, USA (Brown 1948; Leggitt & Cushman 2001). Brues (1927) described analogous associations of extant caddis-fly larval tubes within active thermal springs at Yellowstone National Park. Therefore, the San Agustín examples constitute the oldest known biomounds formed of caddis-fly larval tubes.

The 'pool mat' sinter formed on emergent, adjacent, higher

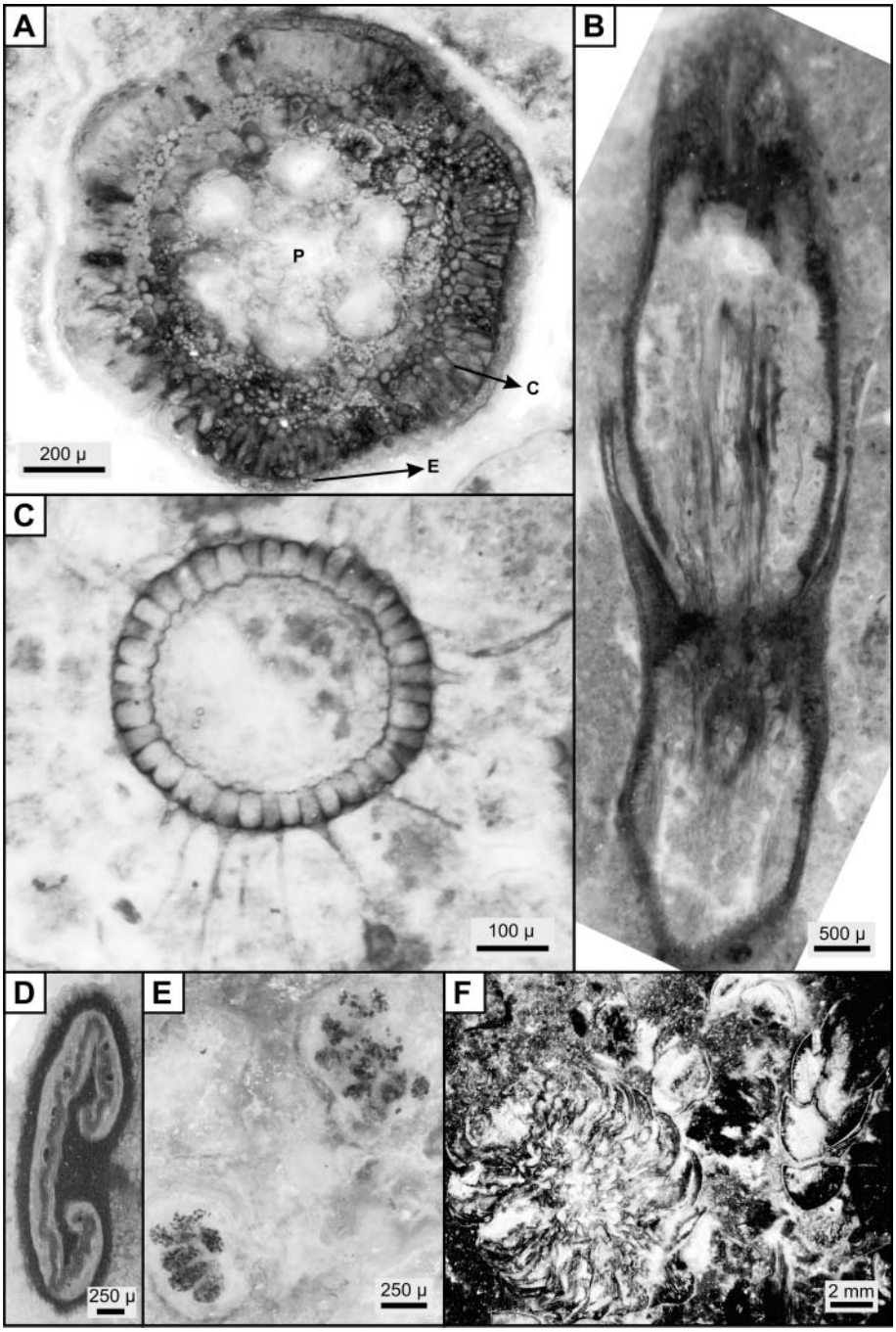


**Fig. 5.** Details of three-dimensionally preserved plant fossils in the San Agustín geothermal system. (**a**) Transverse section of sphenophyte stem illustrating variable preservation of cuticle and epidermis (E), parenchymatous cortex (C) and central pith cavity (P). Northwestern outcrop. (**b**) Longitudinal section of stem illustrating node and internode construction. Central cylinder of vascular tissues in internode segment is surrounded by poorly preserved cortical tissue and/or vallecular canals. Two leaves with sheath-like bases and free apices rise from node at node diaphragm. Northwestern outcrop. (**c**) Transverse section through partially permineralized root illustrating radial arrangement of root hairs. Northwestern outcrop. (**d**) Transverse section through rachis of gleicheniaceous fern with distinctive c-shaped vascular strand. Northwestern outcrop. (**e**) Spore masses found in association with gleicheniaceous fern rachises, Northwestern outcrop. Their morphology and organization suggest the former presence of clusters of sporangia containing trilete spores with concavity between trilete marks. (**f**) Well-preserved conifer cone and *Brachyphyllum*- or *Pagiophyllum*-like conifer foliage in chert. Northern Main outcrop.

sinter terraces (Fig. 1c). This is typified by an irregular, ropy, contorted to fragmental fabric (Figs 2e and m). These textures are comparable with the thick, rubbery microbial mats that grow during the summer months along the margins of and across the surfaces of deep (>1 m), mid-temperature (*c*. 40–55 °C) pools at Orakei Korako, Taupo Volcanic Zone. These mats often become distorted during winter storms with abrupt changes in spring discharge conditions, or fragmented at times of periodic desiccation (e.g. Fig. 2n). In places, the bedding plane surfaces of the 'pool mat' sinter display filamentous 'streamer' fabrics (Fig. 2o), akin to textures (e.g. Fig. 2p) forming in shallow, spring discharge-channels that migrate across mid-temperature sinter aprons in Yellowstone National Park and the Taupo Volcanic Zone today. Undisturbed pool mat fabrics constitute conical tufts (Fig. 3g) of wavy, fine filaments (Fig. 3h), similar to cyanobacterial '*Conophyton*' fabrics developing in Yellowstone National Park and Taupo Volcanic Zone thermal pools (32–59 °C; see Walter *et al.* 1976; Cady & Farmer 1996; Jones *et al*. 2002).

The mid-temperature sinter apron is recognized by the presence of wavy-laminated fabrics with lenticular voids ('bubble mats'; Fig. 2i), in centimetre- to metre-thick bedsets. In places, filaments of probable microbial origin developed as vertical micro-pillars within lenticular cavities (palisade texture, Fig. 3a). Modern and Pleistocene sinters reveal layered bubble mats developed from trapped gases within photosynthesizing cyanobacterial mats that become silicified in mid-temperature channels

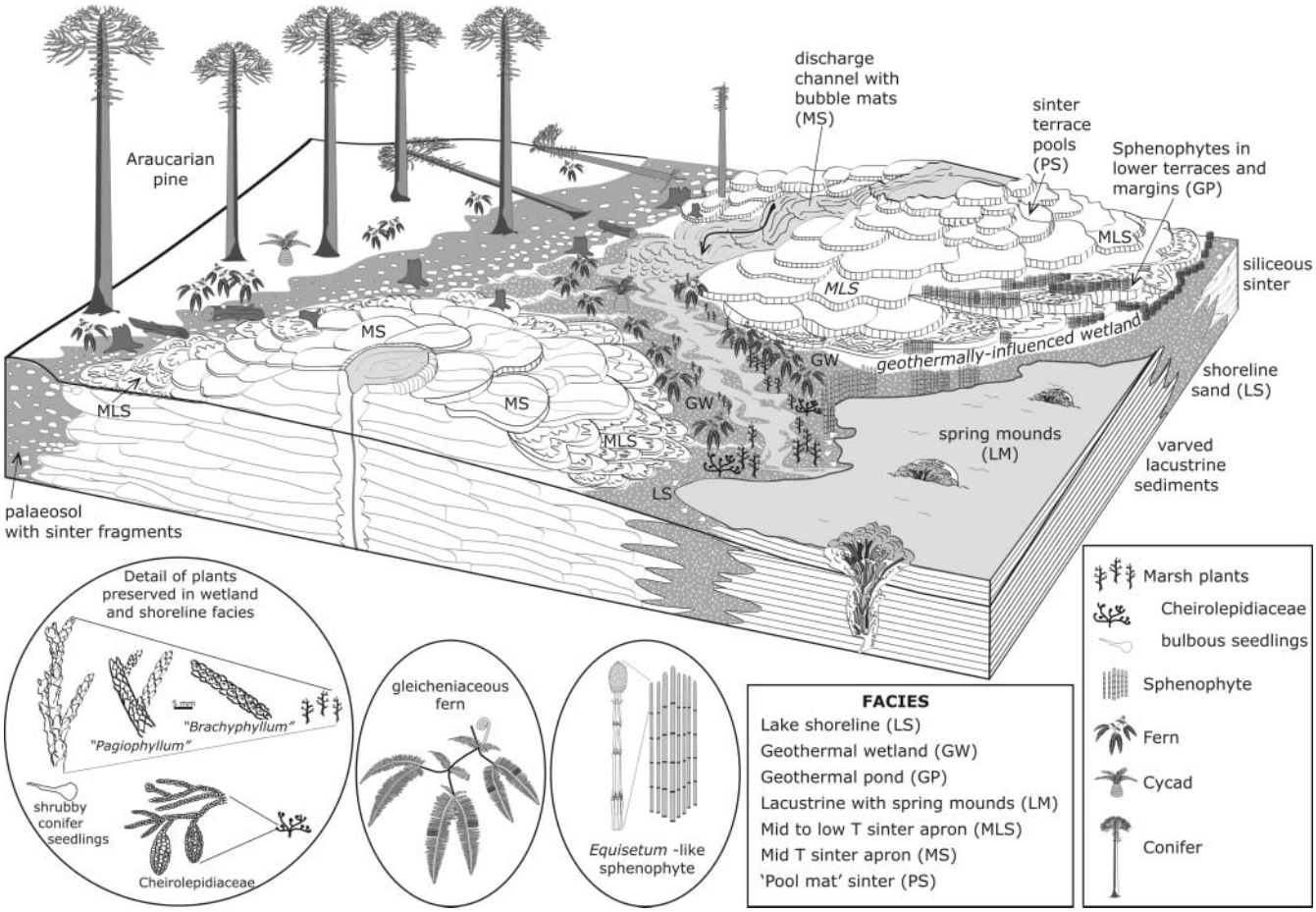


**Fig. 6.** Box diagram illustrating palaeoenvironmental reconstruction of the San Agustín geothermal system. Hot spring-associated facies are labelled, and insets show morphological details of typical marsh and shoreline plants.

(Hinman & Lindstrom 1996; Lynne & Campbell 2003; see Fig. 3b). In contrast, the mid- to low-temperature sinter-apron facies at San Agustín consists of parallel to slightly undulatory, laminated to thinly bedded (millimetre- to centimetre-scale) sinter (Fig. 1f) intercalated, in places, with thin bubble mat horizons, which are inferred as incursions of shallow, migrating, mid-temperature channels across a distal sinter apron.

Silica-rimmed low terraces on the outermost sinter apron (see Fig. 6) enclosed localized supra-apron geothermal ponds (10–20 cm deep, 5–10 m diameter) that were habitats for dense carpets of small sphenophytes (Figs 2j, 5a, b, and 6). Vertical sections through pond-filling sediment record multiple plant growth horizons that contain horizontal rhizomes and roots with intact unicellular hairs (Fig. 5c). Rhizomes link adjacent aerial stems, indicating clonal (vegetative) development, a reproductive strategy observed at some Yellowstone springs at present (Channing & Edwards 2009), and in postulated 'small pond' facies of the Rhynie cherts (Trewin 2001; Fayers & Trewin 2004; Taylor *et al*. 2005). Sporophyte preservation state varies, but near-complete anatomical sections are common (Fig. 5a). Aerial sporophytic stems with tight collars of whorled leaves (Fig. 5b) occur both in life position and as decayed fragments in monotypic litter. Cyprid ostracodes preserved between sphenophyte axes suggest perennially wet, but potentially warm, wetland conditions, as they occur today in springs warmer than 40 °C (e.g. Wickstrom & Castenholz 1985).

Cooler hot-spring margin facies are well represented (Fig. 2a and b), including several outcrops with Lagerstätten-style preservation. They constitute plant-rich cherts formed in geothermally influenced wetlands, and lake shoreline settings. In the geothermally influenced wetland facies, spring-fed marshes extended and prograded across clastic substrates, and a mature conifer forest was engulfed by a growing distal sinter apron (Fig. 6). In similar sites at Yellowstone, lodgepole pines (*Pinus contorta*) die from root flooding. At San Agustín, variously decayed conifer stumps, and fallen branch and trunk fragments (e.g. Fig. 2g), were incorporated into basal sinter deposits, with many coated by microbial laminae and tufted projections (Fig. 3c). Less common gleicheniaceous ferns (Fig. 5d and e) and rare cycads represent local shrubby vegetation. Occurring towards the tops of the same beds, sphenophytes preserved in life position, and in monotypic litter, verify plant succession and partitioning of the flora across the wetland–dryland boundary. The extant sphenophyte genus, *Equisetum*, colonizes similar marginal environments in Icelandic geothermal areas (A.C., personal observation). In associated, microcoprolite-rich fabrics, known to form in thermal streams and shallow ponds at 20–30 °C today (Trewin *et al*. 2003), aquatic and terrestrial arthropod fragments are concentrated (Fig. 4b–e). Finally, lenticular plant-rich cherts, occurring with sharply planar-laminated (varved) siltstone (see Fig. 2k) and hummocky, cross-bedded, fine sandstone, indicate migration of geothermally influenced marsh deposits across a

former lake shoreline (see Fig. 6). In places, varves are directly overlain by a light–dark crenulated fabric inferred as microbial mats (Fig. 2k). Here, the local flora is dominated by shrubby conifers represented by seedlings, stems and articulated foliar axes (see Figs 2l and 5f). Abundant *Classopollis* pollen and male cones (Fig. 5f) indicate the presence of Cheirolepidiaceae, salinity-tolerant elements of Mesozoic floras (Alvin 1982). Plant remains within the lake shoreline facies are enveloped by dense, 'felted' mucilaginous microbial linings and tufted surface projections (Figs 2l and 3c), suggesting wet, marshy conditions of the engulfing siliceous sediments.

## San Agustín sinter analytical data

Oxygen isotope and trace element data for the San Agustín sinter deposit are shown in Table 1. The $\delta^{18}O$ results for San Agustín are in the same range as those for Palaeozoic sinters from Queensland (Cunneen & Sillitoe 1989) and Scotland (Rice & Trewin 1988). They show enrichment in the heavy isotope in comparison with $\delta^{18}O$ from higher temperature epithermal quartz veins: 1.8–15.7‰ for the Deseado Massif (Schalamuk *et al.* 1999*b*). The magnitude of enrichment is different in every sinter deposit because of the local temperature of silica precipitation, the original isotopic composition of the fluid (Ewers 1991) and the intensity of diagenesis and late silica overprinting.

Trace metal analysis (Table 1) of the San Agustín sinter shows typical geochemical signatures for Au, Ag, As and Sb, in the same range as in other ancient surface epithermal deposits. There is a typical depletion of Au and Ag contents (see Sillitoe 1993), with comparatively low As and Sb values.

## Discussion

The San Agustín deposit provides an opportunity to evaluate ecosystem functioning in a Jurassic 'extreme environment'. The fossil plants and animals are similar to those observed from other physicochemically stressed or disturbance-prone habitats, such as ephemeral, evaporation-dominated lakes or saline marshes (see Channing & Edwards 2009). Indeed, comparable fossils are known from the saline lake and bioherm belt of the roughly contemporary (Middle to Late Jurassic) Cañadón Asfalto Formation, Chubut Province, Argentina, *c*. 500 km north of the study area (e.g. Cabaleri & Armella 2005; Escapa *et al*. 2008; Volkheimer *et al*. 2008). Diminutive horsetails preserved at San Agustín further imply a stressed setting, as is also seen by stunted plant growth in active geothermal areas (see Burns 1997), and in the small sphenophyte fossils recorded from ash-fall-associated, ephemeral, shallow pool deposits elsewhere in the Deseado Massif (Middle Jurassic La Matilde Formation; Falaschi *et al*. 2009). Overall, the monotypic plant stands, clonal growth and low floral diversity found at San Agustín are typical features of hot spring vegetation from extant geothermal areas (e.g. Channing & Edwards 2009), and in the fossil record (e.g. Walter *et al*. 1998; Daviero-Gomez *et al*. 2005).

The palaeo-lake at San Agustín accumulated large volumes of volcanic materials (fine, laterally continuous, water-lain tuffs and some coarser ash-fall deposits and epiclastic deposits), as well as geothermal inputs (via lake-floor vent mounds and hot spring areas along lake margins). In the study area, deeper offshore portions of the palaeo-lake are represented by clastic sediments (siltstones and black shales) containing compression fossils of transported fragments of plants (sphenophytes, ferns, bennettitaleans, conifers, lycophytes). A fauna comprising bivalves, gastropods, fish scales, ostracodes and caddis-fly cases suggest relatively normal lake water chemistry for these distal lacustrine strata, but does not preclude oligohaline or alkaline conditions. Extensive evaporite deposits are not evident. However, evaporation of lake water combined with thermal additions and early diagenesis of volcanic deposits potentially enhanced alkalinity and salinity. At the palaeo-lake margins, and in the highest stratigraphic levels of the lacustrine sequence, the presence of areally restricted carbonates and early diagenetic cherts hint at alkaline water chemistry and the presence of playa-like subenvironments.

By virtue of its excellent exposure and clear palaeogeographical and geological framework, the San Agustín deposit also has great potential for deciphering links between ancient volcanism, active tectonism, hot crustal-fluid flow and the birth, growth and death of ancient hot springs. Moreover, diverse affiliated palaeoenvironments with direct modern analogues are evident, some with exceptional fossil preservation. Lagerstätte occur in cherts representing low-temperature or low-energy, wet, geothermally influenced settings adjacent to sinter-apron terraces. These cooler subenvironments suggest ideal conditions under which plants and other organisms both thrived and became silicified in 3D detail (see Trewin 1996, 2001). Hence, the opportunity exists to elucidate regional to micro-scale controls on sinter formation and fossil preservation from the San Agustín deposit. Already a picture is emerging of a Mesozoic geothermal ecosystem that, despite a time difference of some 150 Ma, would not look out of place in Yellowstone or New Zealand today.

We thank the National Geographic Society; INREMI, UNLP and CONICET in Argentina; the Royal Society of London; R. Sims and L. Cotterall at the University of Auckland for technical assistance; and the Marsden Fund Council for government funding, administered by the Royal Society of New Zealand. D. Edwards and E. Jarzembowski are acknowledged for discussions on fossil plants and insects, respectively.

**Table 1.** *Comparative oxygen isotopes and trace metal data from San Agustín and some other Palaeozoic hot spring deposits*

| Location | Age | Description | $\delta^{18}O$ (‰)* | Reference | Au† | Ag† | As† | Sb† | Reference |
|---|---|---|---|---|---|---|---|---|---|
| San Agustín, Argentina | Jurassic | Sinter | 9.8–17.6 ($n = 5$) | This paper | 0.001–0.003 ($n = 3$) | <0.05–0.22 ($n = 3$) | <0.1–78.8 ($n = 3$) | 0.48–3.03 ($n = 3$) | This paper |
| Queensland, Australia | Devonian–Carboniferous | Sinter | 10.9–14.4 ($n = 6$) | Ewers 1991 | <0.008–0.01 ($n = 10$) | <1 ($n = 10$) | <2–50 ($n = 10$) | 4–13 ($n = 10$) | Cunneen & Sillitoe 1989 |
| Rhynie, Scotland | Devonian | Chert | 13.1–16.5 ($n = 13$) | Rice *et al*. 1995 | 0.05–0.18 ($n = 4$) | <2 ($n = 4$) | 15–66 ($n = 4$) | <5–22 ($n = 4$) | Rice & Trewin 1988 |

* Stable Isotope Laboratory of the University of Salamanca, Spain.
† Aqua regia digestion and inductively coupled plasma mass spectrometry determination at Actlabs Ltd., Canada. All values in ppm.

## References


Alvin, K.L. 1982. Cheirolepidiaceae: Biology, structure and paleoecology. *Review of Palaeobotany and Palynology*, **37**,0.5274, L.I. & Trewin, N.H. 2003. An Early Devonian arthropod fauna from the Windyfield Cherts, Aberdeenshire, Scotland. *Palaeontology*, **46**, 467–509.

Brown, R.W. 1948. Algal pillars miscalled geyser cones. *Annual Report of the Board of Regents of the Smithsonian Institution*, June 1948, 277–290.

Brues, C.T. 1927. Animal life in hot springs. *Quarterly Review of Biology*, **2**, 181–203.

Burns, B. 1997. Vegetation change along a geothermal stress gradient at the Te Kopia steamfield. *Journal of the Royal Society of New Zealand*, **27**, 279–294.

Cabaleri, N.G. & Armella, C. 2005. Influence of a biohermal belt on the lacustrine sedimentation of the Cañadón Asfalto Formation (Upper Jurassic, Chubut province, Southern Argentina. *Geologica Acta*, **3**, 205–214.

Cady, S.L. & Farmer, J.D. 1996. Fossilisation processes in siliceous thermal springs: Trends in preservation along thermal gradients. *In:* Brock, G.R. & Goode, J.A. (eds) *Evolution of Hydrothermal Ecosystems on Earth (and Mars?)*. Ciba Foundation Symposium Series, **202**, 150–170.

Campbell, K.A., Sannazzaro, K., Rodgers, K.A., Herdianita, N.R. & Browne, P.R.L. 2001. Sedimentary facies and mineralogy of the Late Pleistocene Umukuri silica sinter, Taupo Volcanic Zone, New Zealand. *Journal of Sedimentary Research*, **71**, 728–747.

Channing, A. & Edwards, D. 2009. Silicification of higher plants in geothermally influenced wetlands: Yellowstone as a Lower Devonian Rhynie analog. *Palaios*, **24**, 505–521.

Channing, A., Edwards, D. & Sturtevant, S. 2004. A geothermally influenced wetland containing unconsolidated geochemical sediments. *Canadian Journal of Earth Sciences*, **41**, 809–827.

Channing, A., Zamuner, A.B. & Zúñiga, A. 2007. A new Middle–Late Jurassic flora and hot spring chert deposit from the Deseado Massif, Santa Cruz province, Argentina. *Geological Magazine*, **144**, 401–411.

Cunneen, R. & Sillitoe, R.H. 1989. Palaeozoic hot spring sinter in the Drummond basin, Queensland, Australia. *Economic Geology*, **84**, 135–142.

Daviero-Gomez, V., Kerp, H. & Hass, H. 2005. *Nothia aphylla*: The issue of clonal development in early land plants. *International Journal of Plant Sciences*, **166**, 319–326.

Echeveste, H. 2005. Travertinos y jasperoides de Manantial Espejo, un ambiente de hot spring Jurásico, Macizo del Deseado, provincia de Santa Cruz. *Latin American Journal of Sedimentology and Basin Analysis*, **12**, 33–48.

Edwards, D., Kerp, H. & Hass, H. 1998. Stomata in early land plants: An anatomical and ecophysiological approach. *Journal of Experimental Botany*, **49**, 255–278.

Engel, M.S. & Grimaldi, D.A. 2004. New light shed on the oldest insect. *Nature*, **427**, 627–630.

Escapa, I.H., Sterli, J., Pol, D. & Nicoli, L. 2008. Jurassic tetrapods and flora of Cañadón Asfalto Formation in Cerro Cóndor area, Chubut Province. *Revista de la Asociación Geológica Argentina*, **63**, 613–624.

Ewers, G.R. 1991. Oxygen isotopes and the recognition of siliceous sinters in epithermal ore deposits. *Economic Geology*, **56**, 173–178.

Falaschi, P., Zamuner, A.B. & Foix, N. 2009. Una nueva Equisetaceae fértil de la Formación La Matilde, Jurásico Medio, Argentina, *Ameghiniana*, **46**, 263–272.

Farmer, J.D. 2000. Hydrothermal systems: Doorways to early biosphere evolution. *GSA Today*, **10**, 1–9.

Fayers, S.R. & Trewin, N.H. 2004. A review of the palaeoenvironments and biota of the Windyfield chert. *Transactions of the Royal Society of Edinburgh: Earth Sciences*, **94**, 325–339.

Guido, D. & Schalamuk, I.B. 2003. Genesis and exploration potential for low sulfidation epithermal deposits in the Deseado Massif, Argentinean Patagonia. *In:* Eliopoulos, D., *et al*. (eds) *Mineral Exploration and Sustainable Development, 1*. Balkema, Rotterdam, 493–496.

Guido, D., De Barrio, R. & Schalamuk, I. 2002. La Marciana Jurassic sinter—implications for exploration for epithermal precious-metal deposits in the Deseado Massif, southern Patagonia, Argentina. *Transactions, Institution of Mining and Metallurgy* (*Section B*: *Applied Earth Science*), **111**, 106–113.

Guido, D.M. & Campbell, K.A. 2009. Jurassic hot-spring activity in a fluvial setting at La Marciana, Patagonia, Argentina. *Geological Magazine*, **146**, 617–622.

Halley, R.B. 1976. Textural variation within Great Salt Lake algal mounds. *In:* Walter, M.R. (ed.) *Stromatolites*. Developments in Sedimentology, **20**, 435–445.

Hinman, N.W. & Lindstrom, R.F. 1996. Seasonal changes in silica deposition in hot spring systems. *Chemical Geology*, **132**, 237–246.

Jones, B., Renaut, R.W. & Rosen, M.R. 1998. Microbial biofacies in hot-spring sinters: A model based on Ohaaki Pool, North Island, New Zealand. *Journal of Sedimentary Research*, **68**, 413–434.

Jones, B., Renaut, R.W., Rosen, M.R. & Ansdell, K.M. 2002. Coniform stromatolites from geothermal systems, North Island, New Zealand. *Palaios*, **17**, 84–103.

Kenrick, P. & Crane, P.R. 1997. The origin and early evolution of plants on land. *Nature*, **389**, 33–39.

Konhauser, K.O., Phoenix, V.R., Bottrell, S.H., Adams, D.G. & Head, I.M. 2001. Microbial–silica interactions in Icelandic hot spring sinter: Possible analogues for some Precambrian siliceous stromatolites. *Sedimentology*, **48**, 415–433.

Leggitt, V.L. & Cushman, R.A., Jr. 2001. Complex caddisfly-dominated bioherms from the Eocene Green River Formation. *Sedimentary Geology*, **145**, 377–396.

Lynne, B.Y. & Campbell, K.A. 2003. Diagenetic transformations (opal-A to quartz) of low- and mid-temperature microbial textures in siliceous hot-spring deposits, Taupo Volcanic Zone, New Zealand. *Canadian Journal of Earth Sciences*, **40**, 1679–1696.

Marchionni, D.S., De Barrio, R.E., Tessone, M.O., Del Blanco, M.A. & Echeveste, H.J. 1999. Hallazgo de estructuras estromatolíticas jurásicas en el Macizo del Deseado, provincial de Santa Cruz. *Revista de la Asociación Geológica Argentina*, **54**, 173–176.

Paik, I.S. 2005. The oldest record of microbial–caddisfly bioherms from the Early Cretaceous Jinju Formation, Korea: Occurrence and palaeoenvironmental implications. *Palaeogeography, Palaeoclimatology, Palaeoecology*, **218**, 301–315.

Pankhurst, R.J., Leat, P.T., Sruoga, P., Rapela, C.W., Marquez, M., Storey, B.C. & Riley, T.R. 1998. The Chon Aike province of Patagonia and related rocks in West Antarctica: A silicic large igneous province. *Journal of Volcanology and Geothermal Research*, **81**, 113–136.

Pankhurst, R.J., Riley, T.R., Fanning, C.M. & Kelley, S.R. 2000. Episodic silicic volcanism in Patagonia and the Antarctic Peninsula: Chronology of magmatism associated with the break-up of Gondwana. *Journal of Petrology*, **41**, 605–625.

Rice, C.M. & Trewin, N.H. 1988. A Lower Devonian gold-bearing hot spring system, Rhynie, Scotland. *Transactions, Institution of Mining and Metallurgy* (*Section B*: *Applied Earth Science*), **97**, B141–B144.

Rice, C.M., Ashcroft, W.A., Batten, D.J., *et al*. 1995. A Devonian auriferous hot spring system, Rhynie, Scotland. *Journal of the Geological Society, London*, **152**, 229–50.

Riley, T.R., Leat, P.T., Pankhurst, R.J. & Harris, C. 2001. Origin of large volume rhyolitic volcanism in the Antarctic Peninsula and Patagonia by crustal melting. *Journal of Petrology*, **42**, 1043–1065.

Schalamuk, I., Zubia, M., Gennini, A. & Fernandez, R.R. 1997. Jurassic epithermal Au–Ag deposits of Patagonia, Argentina. *Ore Geology Reviews*, **12**, 173–186.

Schalamuk, I., Guido, D., De Barrio, R. & Fernandez, R. 1999*a*. Hot spring structures from El Macanudo–El Mirasol area, Deseado Massif, Argentina. *In:* Stanley, C.J., *et al*. (eds) *Mineral Deposits: Processes to Processing, 1*. Balkema, Rotterdam, 577–580.

Schalamuk, I.B., De Barrio, R.E., Zubia, M.A., Gennini, A. & Echeveste, H. 1999*b*. Provincia Auroargentífera del Deseado. *In:* Zappettini, E.O. (ed.) *Recursos Minerales de la República Argentina, 35*. Instituto de Geología y Recursos Minerales SEGEMAR, Buenos Aires, 1177–1188.

Shear, W.A. & Selden, P.A. 2001. Rustling in the undergrowth: Animals in early terrestrial ecosystems. *In:* Gensel, P.G. & Edwards, D. (eds) *Plants Invade the Land: Evolutionary and Environmental Perspectives*. Columbia University Press, New York, 29–51.

Shock, E.L. 1996. Hydrothermal systems as environments for the emergence of life. *In:* Brock, G.R. & Goode, J.A. (eds) *Evolution of Hydrothermal Ecosystems on Earth (and Mars?)*. Ciba Foundation Symposium Series, **202**, 40–52.

Sillitoe, R.H. 1993. Epithermal models: Genetic types, geometric controls and shallow features. *In:* Kirkham, R.V., Sinclair, W.D., Thorpe, R.I. & Duke, J.M. (eds) *Mineral Deposit Modeling*. Geological Association of Canada, Special Volume, **40**, 403–417.

Simmons, S.F., Keywood, M., Scott, B.J. & Keam, R.F. 1993. Irreversible change of the Rotomahana–Waimangu hydrothermal system (New Zealand) as a consequence of a volcanic eruption. *Geology*, **21**, 643–646.

Stetter, K.O. 1996. Hyperthermophiles in the history of life. *In:* Brock, G.R. & Goode, J.A. (eds) *Evolution of Hydrothermal Ecosystems on Earth (and Mars?)*. Ciba Foundation Symposium Series, **202**, 1–10.

Taylor, J.W. & Berbee, M.L. 2006. Dating divergences in the fungal tree of life: Review with some new analyses. *Mycologia*, **98**, 838–849.

Taylor, T.N., Kerp, H. & Hass, H. 2005. Life history biology of early land plants: Deciphering the gametophyte phase. *Proceedings of the National Academy of Sciences of the USA*, **102**, 5892–5897.

Trewin, N.H. 1996. The Rhynie Cherts: An Early Devonian ecosystem preserved by hydrothermal activity. *In:* Brock, G.R. & Goode, J.A. (eds) *Evolution of Hydrothermal Ecosystems on Earth (and Mars?)*. Ciba Foundation Symposium Series, **202**, 131–149.

Trewin, N.H. 2001. The Rhynie Chert. *In:* Briggs, D.E.G. & Crowther, P. (eds)

*Palaeobiology II*. Blackwell Science, Oxford, 342–346.

Trewin, N.H. & Rice, C.M. (eds) 2004. The Rhynie hot springs system: geology, biota and mineralisation. *Transactions of the Royal Society of Edinburgh, Earth Sciences*, **94**.

Trewin, N.H., Fayers, S.R. & Kelman, R. 2003. Subaqueous silicification of the contents of small ponds in an Early Devonian hot-spring complex, Rhynie, Scotland. *Canadian Journal of Earth Sciences*, **40**, 1697–1712.

Volkheimer, W., Rauhut, O.W.M., Quattrocchio, M.E. & Martinez, M.A. 2008. Jurassic paleoclimates in Argentina, A review. *Revista de la Asociación Geológica Argentina*, **63**, 549–556.

Walter, M.C., Bauld, J. & Brock, T.D. 1976. Microbiology and morphogenesis of columnar stromatolites (*Conophyton, Vacerrilla*) from hot springs in Yellowstone National Park. *In:* Walter, M.R. (ed.) *Stromatolites*. Developments in Sedimentology, **20**, 273–310.

Walter, M.C., Des Marais, D., Farmer, J.D. & Hinman, N.W. 1996. Lithofacies and biofacies of mid-Paleozoic thermal spring deposits in the Drummond Basin, Queensland, Australia. *Palaios*, **11**, 497–518.

Walter, M.R., Mcloughlin, S., Drinnan, A.N. & Farmer, J.D. 1998. Palaeontology of Devonian thermal spring deposits, Drummond Basin, Australia. *Alcheringa*, **22**, 285–314.

White, N.C., Wood, D.G. & Lee, M.C. 1989. Epithermal sinters of Paleozoic age in north Queensland, Australia. *Geology*, **17**, 718–722.

Wickstrom, C.E. & Castenholz, R.W. 1985. Dynamics of cyanobacterial and ostracod interactions in an Oregon hot spring. *Ecology*, **66**, 1024–1041.

Received 9 July 2009; revised typescript accepted 6 October 2009.
Scientific editing by Rob Strachan.